Macromolecules **1982,** *15,* 791–800

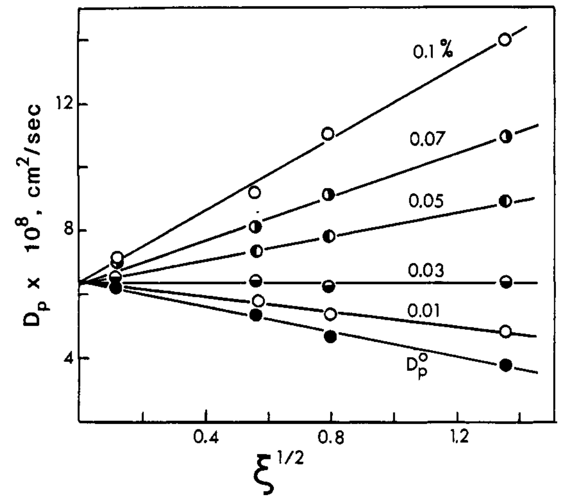

Figure 5. Relationship between D_p and charge density at different polyelectrolyte concentrations above and below the critical concentration (0.03%) in 0.1 M NaBr. The points were taken from the least-squares fits of the data in Figure 1.

critical concentration, which is depicted as a horizontal line, the values of D_p increase with increasing charge density, while below the critical concentration they decrease with increasing charge density, as do the limiting diffusion coefficients depicted in Figure 3. It would appear that below the critical concentration primarily intramolecular interactions dominate, since the trends in the data may be explained in terms of the same arguments that are used at infinite dilution. The reversal in the trends above the critical point may be due to the increased importance of intermolecular interactions with increasing polyelectrolyte concentration, which become dominant above the critical concentration. In view of this behavior, perhaps comparisons of experimental data with limiting laws should be restricted to experiments performed at polyelectrolyte concentrations below 0.03%.

Similar trends to the ones described here may be seen in the diffusion data reported by Nagasawa et al.[26] for NaPSS ($\xi = 2.85$) in aqueous NaBr solutions. The values for D_p for NaPSS increase with increasing polyelectrolyte concentration, with the largest slopes being observed at the lowest concentrations of NaBr. Of particular interest, although not discussed by the authors, the plots of D_p vs. C_p at several NaBr concentrations also exhibit a common point of intersection at 0.03% NaPSS concentration, with the same trends above and below the critical point as with our NaPAM polyelectrolytes. Since both NaPSS and the NaPAM-*y* polyelectrolytes exhibit a critical point at the same concentration, it would appear that, at least for vinylic polyelectrolytes, the critical concentration is independent of the nature of the ionic group. Similar studies with other polyelectrolyte systems should be conducted to verify this.

References and Notes

(1) Ander, P. *ACS Symp. Ser.* **1981**, *No. 150*, Chapter 28.
(2) Ander, P.; Lubas, W. *Macromolecules* **1981**, *14*, 1058.
(3) Ander, P.; Lueng-Louie, L.; Sylvestri, F. *Macromolecules* **1979**, *12*, 1204.
(4) Magdelenat, H.; Turq, P.; Tivan, P.; Menez, R.; Chemla, M.; Driford, M. *Biopolymers* **1979**, *18*, 187.
(5) Magdelenat, H.; Turq, P.; Chemla, M. *Biopolymers* **1974**, *13*, 1535.
(6) Jamieson, A. M.; McDonnell, M. E. *Adv. Chem. Ser.* **1978**, *No. 174*, 163.
(7) Chu, B. *Annu. Rev. Phys. Chem.* **1970**, *21*, 145.
(8) Pecora, R. *Annu. Rev. Biophys. Bioeng.* **1972**, *1*, 257.
(9) Fulmer, A. W.; Benbasat, J. A.; Bloomfield, V. A. *Biopolymers* **1981**, *20*, 1147.
(10) Koene, R. S.; Smit, H. W. J.; Mandel, M. *Chem. Phys. Lett.* **1980**, *74*, 176.
(11) Parthasarathy, N.; Schmitz, K. S. *Biopolymers* **1980**, *19*, 1655.
(12) Chao, D. Y.; Jamieson, A. M. *J. Polym. Sci., Polym. Phys. Ed.* **1980**, *18*, 607.
(13) Lin, S. C.; Lee, W. I.; Schurr, J. M. *Biopolymers* **1978**, *17*, 1041.
(14) Jamieson, A. M.; Presley, C. T. *Int. J. Polym. Mater.* **1976**, *4*, 161.
(15) Kowblansky, M.; Zema, P. *Macromolecules* **1981**, *14*, 166.
(16) Kowblansky, M.; Zema, P. *Macromolecules* **1981**, *14*, 1448.
(17) Kowblansky, M.; Zema, P. *Macromolecules* **1981**, *14*, 1451.
(18) Katchalsky, A. *Pure Appl. Chem.* **1971**, *26*, 327.
(19) Oosawa, F. *J. Polym. Sci.* **1957**, *23*, 421.
(20) Manning, G. S. *Acc. Chem. Res.* **1979**, *12*, 443.
(21) Manning, G. S. *Annu. Rev. Phys. Chem.* **1972**, *23*, 117.
(22) Klein, J.; Conrad, K. *Makromol. Chem.* **1980**, *181*, 227.
(23) Madelkern, L.; Flory, P. J. *J. Chem. Phys.* **1952**, *20*, 212.
(24) Mandelkern, L.; Krigbaum, W. R.; Scheraga, H. A.; Flory, P. J. *J. Chem. Phys.* **1952**, *20*, 1392.
(25) Fox, T. G.; Mandelkern, L. *J. Chem. Phys.* **1953**, *21*, 187.
(26) Suzuki, Y.; Noda, I.; Nagasawa, M. *J. Phys. Chem.* **1969**, *73*, 797.

Second Virial Coefficient of Polydisperse Polymers

Genzo Tanaka and Karel Šolc*

Michigan Molecular Institute, Midland, Michigan 48640. *Received November 24, 1981*

ABSTRACT: The osmotic and light-scattering second virial coefficients, A_2^{OS} and A_2^{LS}, of polydisperse homopolymers are calculated by using the Padé approximant based on the first three coefficients C_k (k = 0, 1, 2) in the cluster series for A_{ij}, the second virial coefficient between two molecules of molecular weights M_i and M_j. The third coefficient C_2 is reevaluated and an error in the earlier result corrected. It is predicted that A_{ij} is always equal to or greater than the arithmetic average of A_{ii} and A_{jj}. In a ternary system, both A_2^{OS} and A_2^{LS} as functions of composition of the mixed homopolymer exhibit a maximum if the ratio of the two molecular weights and the solvent power are high enough. This conclusion is consistent with experimental data. For continuous molecular weight distributions of the Schulz–Zimm and log-normal types, ratios $A_2^{\mathrm{OS}}/A_2^{\mathrm{LS}}$ are greater than unity, in accord with the hard-sphere theory, but contrary to its results they tend to approach some solvent-dependent limit as the polydispersity increases.

I. Introduction

Extensive studies of the second virial coefficient A_2[1,2] of flexible polymers have been done for many years, experimentally and theoretically.[3] Most of them are limited to monodisperse linear polymers and there is no satisfactory theory of A_2[4-12] for a mixture of two monodisperse linear polymers differing only in molecular weight. The Flory–Krigbaum theory[13] and the hard-sphere model[14] by

0024-9297/82/2215-0791$01.25/0

Casassa predict that under certain conditions the osmotic second virial coefficient A_2^{OS} and the light scattering second virial coefficient A_2^{LS} exhibit a maximum as functions of relative compositions of two polymers, as indeed observed experimentally. However, the Flory–Krigbaum theory and its modifications[13,15,16] are less satisfactory[3] for monodisperse systems, and the hard-sphere model is valid only for long polymer molecules in very good solvents.

According to the two-parameter theory[3] of dilute polymer solutions, interactions between two molecules composed of the same chemical units can be expanded in series in terms of the segment–segment interaction parameter β. Such perturbation series are useful only in a very limited range, but recent work[17-19] shows that Padé approximants, based on the first few coefficients of the perturbation theory for chain expansion factors and A_2 of monodisperse linear polymers, give excellent results over the whole range of experimental data. In this paper, we attempt to extend the method to the second virial coefficient for polymers heterogeneous in molecular weight.

In order to obtain Padé approximants for heterogeneous polymers, the first three perturbation coefficients C_k ($k = 0, 1, 2$) for A_{ij}, the second virial coefficient between two molecules of molecular weights M_i and M_j, are required in our treatment. Although the C_k's are reported in the literature,[20,21] we recalculated them since the present treatment depends crucially on their values. We have found that the earlier result[21] for the third coefficient C_2 should be revised. Since the exact formula for C_2 is very complicated, we present it in a simple approximate form based on our numerical work. Highly accurate data for A_2^{OS} and A_2^{LS} are required for obtaining reliable estimates of A_{ij} that could be meaningfully compared to theoretical results. Some rigorous criteria, independent of Padé approximation, for internal consistency of data are presented in section III. These should be helpful for recognizing and discarding measurements that suffer from obvious errors. Some numerical results are presented in section VI and compared with data. Also, the effects of polydispersity on A_2^{OS} and A_2^{LS} are discussed.

II. Basic Equations

We consider a dilute solution containing a set of homopolymer species i differing only in molecular weight in a single solvent.

The osmotic pressure Π and the reciprocal of the Rayleigh ratio R_θ of the solution may be expanded in terms of the total polymer concentration $c = \sum_i c_i$ in the series[1,2]

$$\Pi/cRT = M_n^{-1} + A_2^{OS}c + ... \qquad (1)$$

$$Kc/R_\theta = M_w^{-1} + 2A_2^{LS}c + ... \qquad (2)$$

where R is the gas constant, T is temperature, and K is a constant depending on the optical parameters of the experiment. The number-average (M_n) and weight-average (M_w) molecular weights, expressed in terms of the weight fractions w_i and molecular weights M_i of polymer species i, are

$$M_n = [\sum_i (w_i/M_i)]^{-1} \qquad (3)$$

$$M_w = \sum_i w_i M_i \qquad (4)$$

Similarly, the second virial coefficients observed in osmotic and light-scattering experiments, A_2^{OS} and A_2^{LS}, are given by[2,13,22,23]

$$A_2^{OS} = \sum_{i,j} w_i w_j A_{ij} \qquad (5)$$

$$A_2^{LS} = M_w^{-2} \sum_{i,j} w_i w_j M_i M_j A_{ij} \qquad (6)$$

where A_{ij} represents interactions between a pair of macromolecules i and j at infinite dilution[1,2]

$$A_{ij} = -\frac{N_A}{2M_iM_jV}\int [F_2(i,j) - F_1(i)F_1(j)]\ \mathrm{d}(i)\ \mathrm{d}(j) \qquad (7)$$

Here, N_A is the Avogadro number, V is the volume of the solution, and F_1 and F_2 are the one- and two-body distribution functions[1,2] specifying the conformation of macromolecule(s).

According to the two-parameter theory, A_{ij} is a function of the excluded volume parameter z and the ratio ϵ of molecular weights of the two macromolecules and may be written as[3]

$$A_{12} = \frac{N_A\beta}{2m^2}h(\epsilon,z) \qquad (8)$$

where m is the molecular weight of a polymer segment and β is the binary cluster integral for a pair of segments. For later convenience we use here subscripts 1 and 2 instead of i and j and define ϵ as

$$\epsilon = M_2/M_1 \qquad (9)$$

with

$$M_2 \geq M_1 \qquad (10)$$

When $\epsilon = 1$, eq 8 reduces to the second virial coefficient for a monodisperse polymer, A_{ii}.

The rigorous result for the h function is known only in the series form[20,21]

$$h(\epsilon,z) = 1 - C_1(\epsilon)z + C_2(\epsilon)z^2 - ... \qquad (11)$$

For the heterogeneous case, $M_1 \neq M_2$, the definition of the parameter z is somewhat arbitrary since the perturbation theory yields results only for the products $C_1(\epsilon)z$, $C_2(\epsilon)z^2$, etc. We identify z with z_1, the conventional z parameter for the polymer with lower molecular weight:

$$z \equiv z_1 = (4\pi\langle S^2\rangle_{0,1}/M_1)^{-3/2}m^{-2}M_1^{1/2}\beta \qquad (12)$$

Here $\langle S^2\rangle_{0,1}$ is the unperturbed mean-square radius of gyration for polymer 1.

Based on the first three perturbation coefficients, we obtain a Padé approximant of the h function[18] for a pair of molecules as

$$h(\epsilon,z) = \left(1 + \frac{C_1(\epsilon)}{\gamma}z\right)^{-\gamma} \qquad (13)$$

where

$$\gamma^{-1} = \frac{2C_2(\epsilon)}{C_1^2(\epsilon)} - 1 \qquad (14)$$

Equation 13 with eq 8 then gives A_{12} in our approximation.

It is apparent that the observed second virial coefficients A_2^{OS} and A_2^{LS} can be approximated in two ways differing by the order in which the two operations are carried out: The approximation, eq 13 and 14, can be taken for each pair of molecules separately, and then the resulting A_{ij}'s averaged for the given molecular weight distribution $w(M)$. This method will be referred to as "A_{ij} averaging". Alternately, it is also possible to evaluate A_2^{OS} and A_2^{LS} by first averaging the C_k's of eq 11 for the given $w(M)$, followed by constructing a single Padé approximant. This procedure is more convenient for computation, especially for polymers with more than two components, and shall be termed "C_k averaging".

III. Ternary System

The theory of A_{12} may be examined by observing A_2 for a ternary system consisting of two polymers with molecular weights M_1 and M_2 and a solvent. Since a successful analysis requires data of high accuracy, it is advantageous to have some quantitative criteria enabling us to weed out experimental data with obvious internal inconsistencies. Such rigorous relations can be derived directly from eq 5 and 6.

The functions $A_2^{\mathrm{OS}}(w)$ and $A_2^{\mathrm{LS}}(w)$ exhibit extrema at

$$w_{\mathrm{m}}^{\mathrm{OS}} = (1 + X)^{-1} \tag{15}$$

$$w_{\mathrm{m}}^{\mathrm{LS}} = (1 + \epsilon X)^{-1} \tag{16}$$

where w represents the weight fraction of the higher molecular component 2 in the polymer mixture, the subscript m indicates an extremum, and

$$X = (A_{12} - A_{22})/(A_{12} - A_{11}) \tag{17}$$

If the extremum is observed experimentally, w_{m} should be in the range $0 \leq w_{\mathrm{m}} \leq 1$ and the following criteria should hold (provided that $A_{11} > A_{22}$)

$$A_{11} > A_{22} > A_{12} \qquad \text{for a minimum} \tag{18}$$

$$A_{12} > A_{11} > A_{22} \qquad \text{for a maximum} \tag{19}$$

as was first pointed out by Casassa.[14]

It is noted here that the extremum for A_2^{LS}, if it exists, appears at a very low value of w when ϵ is large. Substituting eq 15 and 16 into eq 5 and 6, we find for a ternary system

$$\begin{aligned} A_{\mathrm{m}} &= A_2^{\mathrm{OS}}(w_{\mathrm{m}}^{\mathrm{OS}}) = A_2^{\mathrm{LS}}(w_{\mathrm{m}}^{\mathrm{LS}}) \\ &= \frac{A_{12}^2 - A_{11}A_{22}}{2A_{12} - A_{11} - A_{22}} \end{aligned} \tag{20}$$

i.e., both methods give the same maximal (or minimal) values of A_2 although at different w's. Thus, for systems with a maximum, A_2^{LS} is larger than A_2^{OS} at low values of w, and only in the rest of the interval the situation is reversed to the more common pattern $A_2^{\mathrm{OS}} > A_2^{\mathrm{LS}}$. Comparing A_{m} with A_{ii}, we have

$$A_{\mathrm{m}} - A_{ii} = \frac{(A_{12} - A_{ii})^2}{2A_{12} - A_{11} - A_{22}} \qquad \text{for } i = 1, 2 \tag{21}$$

From this relation and eq 18 and 19, it is apparent that A_{m} is also the largest (or smallest) of all observed A_2's.

A_2^{LS} is affected especially by the component with higher molecular weight. Therefore, when ϵ is large, the observed A_2^{LS} is close to A_{22} over a wide range of high w values as can be seen from the series

$$A_2^{\mathrm{LS}} = A_{22} + 2(A_{12} - A_{22})(1 - w)(\epsilon w)^{-1} + \ldots \qquad \text{for } \epsilon w \gg 1 \tag{22}$$

Experimentally, the function $A_2^{\mathrm{OS}}(w)$ is always concave downward (i.e., with a negative second derivative).[4-6,8-10,12] In order to find the physical interpretation of this fact, we consider the following thermodynamic relations.

The chemical potential of the solvent, $\Delta\mu_{\mathrm{s}}$, can be described in general as[24-26]

$$\frac{\Delta\mu_{\mathrm{s}}}{RT} = \ln (1 - \phi) + \left(1 - \frac{m}{M_{\mathrm{n}}}\right)\phi + \chi\phi^2 \tag{23}$$

where ϕ is the total volume fraction of the polymer and χ is the generalized Flory–Huggins interaction parameter that depends on T, ϕ, w, pressure, and molecular weights of both polymers. The last term of eq 23 absorbs all the corrections to the classical Flory–Huggins lattice theory,[27,28] including the dilute-solution correction.

The parameter χ may be expanded as[29]

$$\chi = \chi_1 + \chi_2\phi + \chi_3\phi^2 + \ldots \tag{24}$$

The coefficients χ_i can be related to the osmotic virial coefficients A_{i+1}^{OS} as

$$A_{i+1}^{\mathrm{OS}} = \frac{\bar{v}^{i+1}}{V_{\mathrm{s}}}\left(\frac{1}{i + 1} - \chi_i\right) \tag{25}$$

where $\bar{v}$ is the partial specific volume of the polymer, assumed to be independent of molecular weight and concentration, and V_{s} is the molar volume of the solvent. In particular, for a ternary solution χ_1 may be written as

$$\chi_1 = \frac{1}{2} - \frac{V_{\mathrm{s}}}{\bar{v}^2}[(1 - w)^2A_{11} + 2w(1 - w)A_{12} + w^2A_{22}] \tag{26}$$

On the other hand, Fujita and Teramoto[30] showed that for a ternary system, χ of eq 23 can be expressed in terms of polymer composition w as

$$\chi = (1 - w)\chi_{01} + w\chi_{02} + w(1 - w)\chi_{12} \tag{27}$$

From eq 26 and 27 with eq 24, we have

$$\chi_{01}^{\circ} = \tfrac{1}{2} - (V_{\mathrm{s}}/\bar{v}^2)A_{11} \tag{28}$$

$$\chi_{02}^{\circ} = \tfrac{1}{2} - (V_{\mathrm{s}}/\bar{v}^2)A_{22} \tag{29}$$

where the superscript "°" denotes values at infinite dilution corresponding to χ_1 of eq 24. Substituting eq 28 and 29 into eq 26 and dividing by $w(1 - w)$, we obtain

$$\chi_{12}^{\circ} = \frac{V_{\mathrm{s}}}{\bar{v}^2}(A_{11} + A_{22} - 2A_{12}) = -\frac{V_{\mathrm{s}}}{\bar{v}^2}\frac{\partial^2A_2^{\mathrm{OS}}}{\partial w^2} \tag{30}$$

where the second equality is derived from eq 5. Thus, the curvature of A_2^{OS} vs. w plot is proportional to χ_{12}°, and both quantities are of the same sign. It is noted that χ_{12}° is zero only if A_{12} is an arithmetic average of A_{11} and A_{22}. This can happen in some special cases (e.g., for rodlike molecules or for flexible molecules at the Θ point, where A_{ii} is independent of M). However, we are unaware of any case with χ_{12}° being zero when A_{ii} does depend on M.

In the present notation, the free energy of mixing of the solution per unit volume, ΔF_{m}, may be written as[24-26]

$$\begin{aligned} \Delta F_{\mathrm{m}}/RT = (1 - \phi) \ln (1 - \phi) + m\sum_{i=1}^{2}\phi_iM_i^{-1} \ln \phi_i + \\ (1 - \phi)[\chi_{01}^{\circ}\phi_1 + \chi_{02}^{\circ}\phi_2] - \chi_{12}^{\circ}\phi_1\phi_2 + \mathcal{O}(\phi^3) \end{aligned} \tag{31}$$

Therefore, a negative curvature of $A_2^{\mathrm{OS}}(w)$ implies that interactions between macromolecules 1 and 2 are thermodynamically less favorable than those between identical molecules. If A_{12} were the geometric average of A_{11} and A_{22}, χ_{12}° would be positive and A_2^{OS} concave upward. However, no experiment indicates such behavior.

IV. Perturbation Coefficients $C_1(\epsilon)$ and $C_2(\epsilon)$

$C_1(\epsilon)$ has been evaluated by Yamakawa and Kurata.[20] The result is

$$C_1(\epsilon) = \frac{16}{3}(1 + \epsilon^{1/2}) - \frac{32}{15\epsilon}[(1 + \epsilon)^{5/2} - \epsilon^{5/2} - 1] \tag{32}$$

The evaluation of $C_2(1)$ is not trivial and its value has been several times revised by various authors.[31-34] The long history of this effort is reviewed by Tagami and Casassa,[21] who calculated $C_2(\epsilon)$ for two chains of different lengths and reported the most recent correction to $C_2(1)$. Since their numerical values of $C_2(\epsilon)$ seemed to us inconsistent with their asymptotic formula for $\epsilon \to \infty$, and, on the other hand,

Table I
Comparison of Numerical Values of the Coefficient $C_2(\epsilon)$ Evaluated by Three Different Equations

ϵ	exact	approx closed eq 33	asymptotic eq B3
1.0	13.927	13.900	9.1250
1.5	16.923	16.816	12.948
2.0	19.249	19.125	15.804
2.5	21.159	21.035	18.091
3.0	22.785	22.665	20.000
3.5	24.201	24.089	21.640
4.0	25.458	25.354	23.079
4.5	26.588	26.491	24.360
5.0	27.616	27.526	25.517
5.5	28.558	28.476	26.570
6.0	29.429	29.353	27.538
6.5	30.238	30.168	28.432
7.0	30.994	30.930	29.265
7.5	31.704	31.645	30.043
8.0	32.373	32.318	30.774
8.5	33.005	32.955	31.462
9.0	33.605	33.559	32.113
9.5	34.176	34.134	32.731
10.0	34.720	34.682	33.319
11.0	35.737	35.706	34.415
12.0	36.674	36.649	35.419
13.0	37.542	37.522	36.346
14.0	38.351	38.336	37.208
15.0	39.108	39.097	38.012
16.0	39.819	39.812	38.766
17.0	40.491	40.488	39.476
18.0	41.127	41.127	40.147
19.0	41.730	41.733	40.783
20.0	42.305	42.311	41.387
25.0	44.826	44.843	44.027
30.0	46.910	46.935	46.198
35.0	48.687	48.717	48.041
40.0	50.237	50.272	49.643
45.0	51.610	51.650	51.061
50.0	52.846	52.887	52.332
60.0	54.995	55.040	54.537
70.0	56.821	56.870	56.408
80.0	58.411	58.463	58.033
90.0	59.818	59.872	59.468
100.0	61.082	61.136	60.755
200.0	69.455	69.525	69.262
300.0	74.406	74.480	74.267
400.0	77.986	78.012	77.829

the results of the Padé approximation are sensitive to the value of $C_2(\epsilon)$, we decided to recalculate this coefficient. After a laborious calculation, one of the five integrals to be evaluated (I_2 in Tagami–Casassa notation) was found to contain an error, which even for $\epsilon = 1$ amounts to about a 2.5% correction to the value of C_2. Since by our methods I_2 is reduced to single integrals only, it can be evaluated more easily and very accurately. The correct result for I_2 is given in Appendix A.

The rigorous result for $C_2(\epsilon)$ is very complicated and far from convenient. With the aid of the asymptotic formulas and numerical values (Appendices B and C), we approximate $C_2(\epsilon)$ by a simpler form:

$$C_2(\epsilon) \approx \pi(4 \ln \epsilon - 1) + \frac{16}{3} + \left(\frac{104}{15} + \frac{36}{5\epsilon^{1/2}}\right)[(1 + \epsilon)^{3/2} - \epsilon^{3/2} - 1]\epsilon^{-1} \quad \text{for } \epsilon \geq 1 \qquad (33)$$

Numerical values of $C_2(\epsilon)$ evaluated from three formulas (exact, eq 33, and the first three terms of the asymptotic formula, eq B3) are compared in Table I. The maximal relative deviation of eq 33 from the exact value, observed around $\epsilon = 2$, is very small (~0.7%). Thus, eq 33 may be regarded as a very good approximation to $C_2(\epsilon)$.

V. Polymers with Continuous Molecular Weight Distribution

It is worthwhile to study the effects of heterogeneity in molecular weight on the observed A_2, since polymers are always mixtures of molecular species of different sizes. So far there have been only a few such studies: treatment based on the smooth-density model by Flory–Krigbaum,[13] the first-order perturbation theory result by Yamakawa and Kurata,[20] and the hard-sphere approximation by Casassa.[14] The results of the above studies do not seem satisfactory; the latter two are limited by their design to a restricted interval of z and/or ϵ, while the first one[13] does not yield good results even for monodisperse polymers.

As noted in section II, the Padé approximant method can be applied in two ways: one, for A_{12} (A_{ij} averaging); two, for the observed A_2 (C_k averaging). In this study we chose the C_k-averaging method, which for ternary systems yields results more consistent with available experimental data than the A_{ij}-averaging method.

It is convenient to express A_2^{OS} and A_2^{LS} in terms of z_n or z_w, defined as

$$z_w = (4\pi\langle S^2\rangle_{0,w}/M_w)^{-3/2} m^{-2} M_w^{1/2} \beta \qquad (34)$$

$$z_n = (M_n/M_w)^{1/2} z_w \qquad (35)$$

where $\langle S^2\rangle_{0,w}$ is the unperturbed mean-square radius for the monodisperse polymer of molecular weight M_w. A_2^{OS} and A_2^{LS} may be written in the same form as eq 8

$$A_2^{\mathrm{EX}} = \frac{N_A \beta}{2m^2} h^{\mathrm{EX}}(z_w) \qquad (36)$$

and the perturbation coefficients C_k^{EX} for $h^{\mathrm{EX}}(z_w)$ are given by

$$C_{k,w}^{\mathrm{EX}} = \int\int w_i w_j \left(\frac{M_i M_j}{M_w^2}\right)^D \left[\frac{\mathrm{Min}\,(M_i,M_j)}{M_w}\right]^{k/2} \times C_k\left[\frac{\mathrm{Max}\,(M_i,M_j)}{\mathrm{Min}\,(M_i,M_j)}\right] \mathrm{d}M_i\, \mathrm{d}M_j \qquad (37)$$

where $D = 0$ for EX = OS and $D = 1$ for EX = LS. The function $h^{\mathrm{EX}}(z_w)$ required for eq 36 is calculated from eq 13 and 14 with $C_k(\epsilon)$ replaced by $C_{k,w}^{\mathrm{EX}}$.

We choose two types of molecular weight distribution functions for examination. One is the Schulz–Zimm distribution:[35,36]

$$w_{\mathrm{SZ}}(M) = \frac{y^{h+1}}{\Gamma(h+1)} M^h e^{-yM} \qquad (38)$$

with

$$y = \frac{h}{M_n} = \frac{h+1}{M_w} = \frac{h+2}{M_z} = \ldots \qquad (39)$$

and the other is the log-normal distribution:[37]

$$w_{\mathrm{LN}}(M) = \frac{1}{(2\pi)^{1/2}\sigma M} \exp\left[-\frac{\ln^2 (M/M_m)}{2\sigma^2}\right] \qquad (40)$$

with

$$M_m = (M_n M_w)^{1/2} \qquad (41)$$

$$\exp(\sigma^2) = M_w/M_n = M_z/M_w = \ldots \qquad (42)$$

M_z is the z-average molecular weight.

The coefficient C_1^{EX} for the Schulz–Zimm distribution has been obtained earlier by Yamakawa and Kurata.[20] The other coefficients are reduced to single integrals and

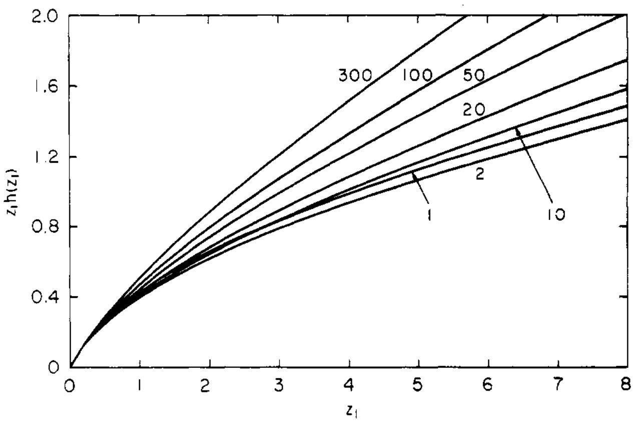

Figure 1. $z_1h(\epsilon,z_1)$ plotted against z_1 for the indicated values of chain length ratio $\epsilon = M_2/M_1$.

evaluated by the $2N$-point Gaussian quadrature.[38] The infinite interval for quadrature is divided into two regions (0,1) and (1,∞), with the latter converted to the finite interval (0,1) by the transformation $y = x^{-1}$. For $N = 16$, 32, and 64, the calculated values agree within 0.01%.

VI. Results and Discussion

First we revise A_2 theory for monodisperse polymers. As indicated in Table I, the exact value of $C_2(1)$ is

$$C_2(1) = 13.9278 \tag{43}$$

which differs from the Tagami–Casassa value 14.278 by about 2.5%. With this correct value, the Padé approximant for the h function proposed by Tanaka[18] is revised as

$$h(1,z) = (1 + 6.856z)^{-0.418} \tag{44}$$

The contribution of exclusively intermolecular interactions to C_2, denoted as C_2^0, is useful in some theoretical considerations.[3,34,39] Its corrected value is

$$C_2^0(1) = 8.8511 \tag{45}$$

Since both C_2 and C_2^0 are modified by the same amount, the first-order coefficient of the expansion factor α^{*3} of one polymer molecule in contact with another remains unchanged, and thus we still may assume that α^* is equal to the expansion factor α_S for the mean-square radius. Then the Yamakawa–Kurata formula[3,34,39] for the h function is revised as

$$\bar{z}h(\bar{z}) = \frac{1 - (1 + 3.537\bar{z})^{-0.620}}{2.193} \tag{46}$$

with

$$\bar{z} = z/\alpha_S^3 \tag{47}$$

It is interesting to note that the revised formulas, eq 44 and 46, give smaller values of h than the old ones and agree better with experimental data for larger values of z.

Next we turn to the question of maxima in A_2 observed for ternary systems. In Figure 1, numerical values of $z_1h(\epsilon,z_1)$ are plotted for several values of ϵ. At the origin, all the curves have an identical slope of unity and a negative second derivative $-2C_1(\epsilon)$ whose magnitude monotonously increases with ϵ. Outside the interval of very small z_1's, however, the quantity z_1h as a function of ϵ (at constant z_1) exhibits a minimum; i.e., it increases with ϵ in the range of higher ϵ values. For any given ϵ this behavior leads to the existence of a threshold value z_1^* at which $z_1^*h(1,z_1^*) = z_1^*h(\epsilon,z_1^*)$. For $z_1 > z_1^*$, we have then always $h(\epsilon,z_1) > h(1,z_1)$, and consequently also $A_{12} > A_{11}$; i.e., a maximum is expected in the composition dependence of observed A_2. The higher is ϵ, the smaller is the threshold value z_1^*. In Figure 2, the domain with expected maxima in A_2 is located above the solid line.

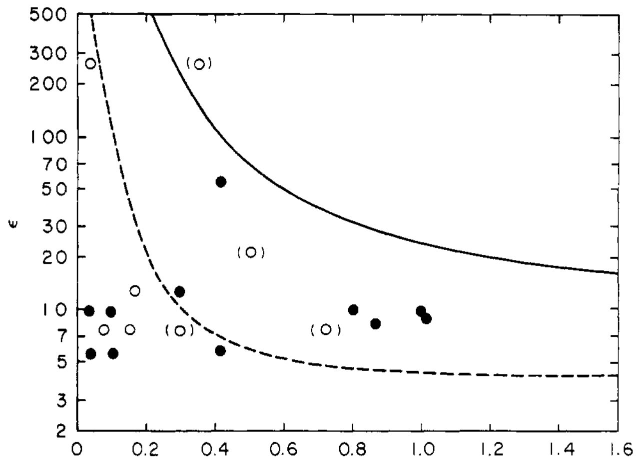

Figure 2. Comparison of theory with experiment. The two curves indicate the predicted lower bounds above which a maximum in functions $A_2^{OS}(w)$ and $A_2^{LS}(w)$ should exist. The solid and broken lines correspond to the A_{ij}-averaging and C_k-averaging methods, respectively. Experimental points: (●) if a maximum has been reported;[4-6,8,12] (O) otherwise.[7,9-11] The open circles with parentheses indicate cases where a maximum might have been overlooked.[7,10,11]

As indicated earlier, the Padé approximant method can also be applied directly to the observed A_2 rather than to A_{12}. In this case, the threshold values z_1^* become smaller, and the corresponding curve in Figure 2 moves down (dashed line). The discrepancy between the two curves, of course, reflects the extent of approximation in the Padé approximant method.

In order to compare the above results with experiment, one needs z_1 values for experimental data. While the unperturbed dimensions are directly measurable, the binary cluster integral β is not and can be arrived at only indirectly. One practical method to determine β is to use the Stockmayer–Fixman plot.[40] The initial slope of the plot with the modified coefficient[41] yields[3,42] reliable values of β. Near the Θ temperature, β may also be estimated[43] from the temperature dependence of A_2. The parameters used in this work are summarized in Table II.[8,43-53]

A solid circle is plotted in Figure 2 for systems with a reported maximum, whereas an open circle indicates that no maximum was observed. It is our belief, however, that in some of these latter cases the maximum just may have been overlooked. This is particularly true of results based only on light-scattering data where the maximum (if present) appears at a relatively low value of w (eq 16). Unless such a low composition range is investigated, no maximum can be observed. In Figure 2, the points corresponding to such studies are enclosed in parentheses. Keeping in mind the relatively large experimental error in determinations of A_2, the agreement between experiment and the C_k-averaging theory (dashed curve) seems quite reasonable. The approximation based on A_{ij} averaging, on the other hand, shifts the boundary between systems with and without maxima to too high values of z_1 and ϵ (solid line).

Numerical values calculated for the observed A_2 by the C_k-averaging method are shown in Figures 3 and 4. The choice of parameters is such that the two graphs correspond to polystyrene ($M_1 = 1 \times 10^6$) in benzene and methyl ethyl ketone, respectively. A_2^{LS} is indicated by a dashed line, whereas A_2^{OS} is shown as a solid line. The numbers attached to the curves represent ϵ. In both solvents curves

Table II
Values of β and $\langle S^2\rangle_0/M$ for Several Polymer-Solvent Systems

polymer	solvent	T, °C	$\beta \times 10^{24}$, cm^3	$\langle S^2\rangle_0/M \times 10^{18}$, (cm^2 mol)/g	ref
polystyrene	benzene	25, 30	34	8.8	43-47
	toluene	25, 30	31	8.8	45, 47
	methyl ethyl ketone	22	4.0	8.8	47, 48
	cis-decalin	12-80	$91(1 - \Theta/T)$	7.2	43
poly(α-methylstyrene)	toluene	25	32	8.2	47, 49
	cyclohexane	35-50	$63(1 - \Theta/T)$	9.1	8
polyisobutylene	cyclohexane	30	14	9.5	47, 50
poly(methyl methacrylate)	methyl ethyl ketone	25	10	6.4	51
	acetone	25	7.1	6.4	51-53

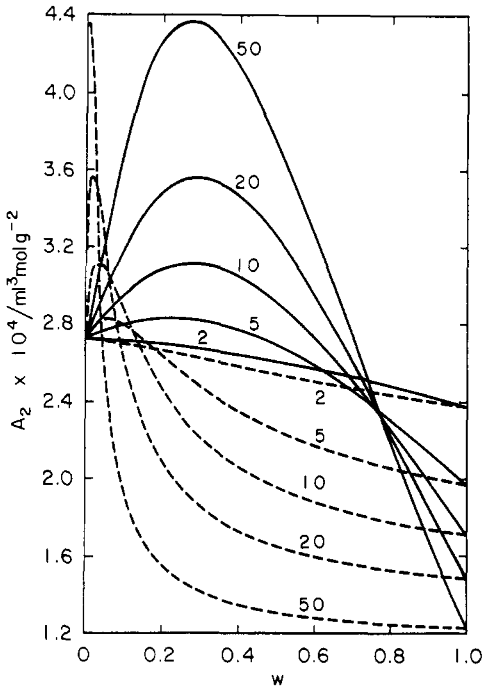

Figure 3. Dependence of A_2^{OS} (—) and A_2^{LS} (---) on w calculated for polystyrene in benzene at 25 and 30 °C. The numbers attached to the curves represent ϵ with $M_1 = 10^6$ fixed.

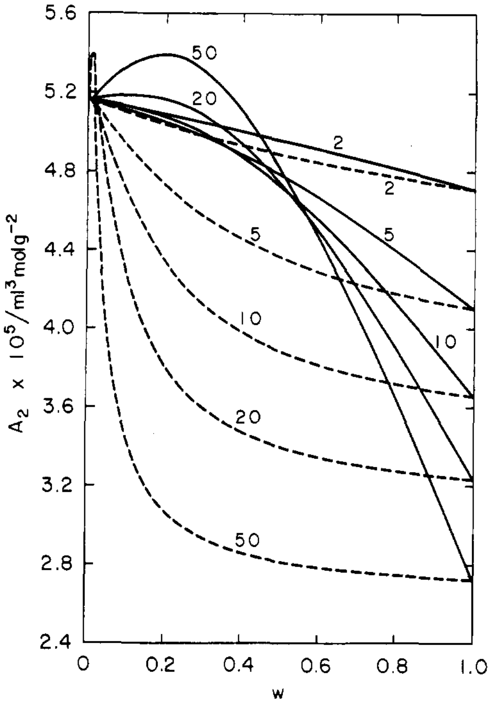

Figure 4. Dependence of A_2^{OS} and A_2^{LS} on w calculated for polystyrene in methyl ethyl ketone at 22 °C. The curves and numbers have the same meaning as in Figure 3.

do show maxima if ϵ is sufficiently high. In a good solvent (benzene), however, the maxima are more pronounced, reaching values much larger than A_{11} (66% higher for ϵ = 50). In a poor solvent, on the other hand, the maxima deviate from A_{11} by just 5% at most, which is well within the experimental error of A_2 measurement. With decreasing M_1 (smaller z_1), the tendency to form a maximum diminishes. In no case have we observed a function $A_2^{\mathrm{OS}}(w)$ with a positive curvature.

Another feature of the graphs is that for large values of w and ϵ, A_2^{LS} is nearly equal to A_{22}. Similar behavior has been observed experimentally by Utiyama, Tagata, and Kurata[9] for polystyrene in methyl ethyl ketone ($\epsilon = 12$, $M_1 = 16 \times 10^4$) and by Suzuki[11] for polystyrene in benzene and in methyl ethyl ketone ($\epsilon = 260$, $M_1 = 1 \times 10^4$). This behavior is just a consequence of weighting for A_2^{LS} (eq 6) and is substantiated by eq 22, regardless of the magnitude of the three coefficients A_{11}, A_{22}, and A_{12}. The latter author[11] also claimed that A_2^{LS} exhibits a minimum for his systems. We believe that this interpretation of his data is erroneous since the results for A_{12} clearly depend on the mixture composition w.

We also view with suspicion the experimental data of Kato, Miyaso, and Nagawasa,[8] who reported having observed maxima in A_2^{LS} for mixtures of two poly(α-methylstyrene) fractions in cyclohexane at 40 and 50 °C. None of the theories, including the present one, could explain existence of a maximum near the Θ temperature (cf. Figure 2). In fact, analysis of their data (using A_2^{LS} and β reported in their paper) yields a function $h(\epsilon,z_1)$ greater than unity (1.2–2.0), which is physically impossible for a positive β with repulsive interactions. This inconsistency is not due to their method of β evaluation from the temperature dependence of A_2, a method which is known to overestimate β if applied over too wide a range of temperatures. With lowered values of β, the h function would be even higher. The data of Kato et al. are also contrary to findings of Wallace and Casassa,[10] who studied similar regions of the (z_1,ϵ) map for a mixture of polystyrene in *cis*-decalin at 24.6, 40, and 80 °C. The latter authors have not observed any maxima in A_2^{LS}, and their values of h remain less than unity even after β is modified. Further, Kato et al.'s data for monodisperse systems show $A_{11} < A_{22}$ for $T < \Theta$. However, this leads to $\chi_{01} > \chi_{02}$ (cf. eq 28 and 29) and, consequently, to $(\Delta F_{\mathrm{m}})_1 > (\Delta F_{\mathrm{m}})_2$ (cf. analogue of eq 31 for a binary system). This is inconsistent with higher solubility of lower molecular weight species 1, compared to that of higher molecular weight species 2.

Expansion of eq 30 around $z = 0$ leads to the relation

$$\chi_{12}^{\circ} = \frac{N_{\mathrm{A}}}{16\pi^{3/2}(\langle S^2\rangle_{0,1}/M_1)^{3/2}}\,\frac{\beta^2}{m^4}\,\frac{V_{\mathrm{s}}}{\bar{v}^2} \times [2C_1(\epsilon) - (1 + \epsilon^{1/2})C_1(1)]M_1^{1/2} \le 0 \qquad (48)$$

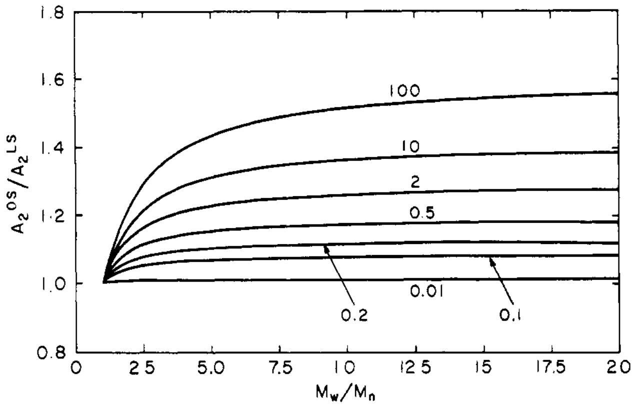

Figure 5. A_2^{OS}/A_2^{LS} plotted against M_w/M_n for polymers with a Schulz-Zimm distribution. The attached numbers indicate values of z_w.

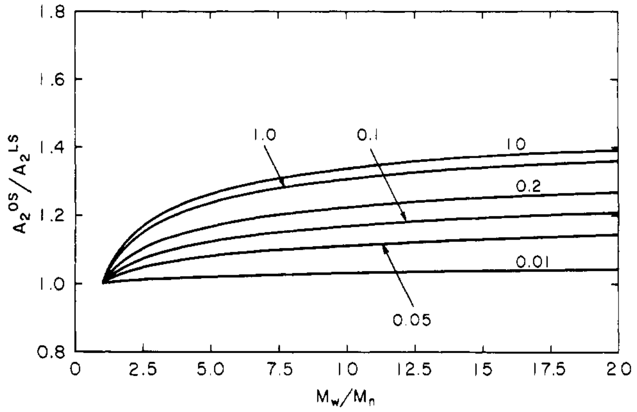

Figure 6. A_2^{OS}/A_2^{LS} plotted against M_w/M_n for polymers with a log-normal distribution. The attached numbers indicate values of z_w.

which predicts χ_{12}° negative, except for $T = \Theta$, where $\chi_{12}^\circ = 0$. This agrees with our results as well as with experiment for $T > \Theta$, as mentioned above. Below the Θ point, Fujita and Teramoto[30] in their study of cloud point curves and critical points for polystyrene in cyclohexane found also a negative value of χ_{12}° (although their data were probably obtained at concentrations higher than those relevant for our work). The negative sign would also be consistent with splitting of a ternary solution into three phases (documented both experimentally[54] and theoretically[55]) when the ratio of chain lengths of the two polymer components exceeds a certain limit. Therefore, a negative χ_{12}° seems to be quite general. It is unlikely that a positive curvature or a minimum of $A_2^{OS}(w)$ and $A_2^{LS}(w)$ would appear or that A_{12} would equal the geometric average of A_{11} and A_{22}. Molecular weight dependence of χ_{12}° near Θ has not been yet studied, but it might be worthwhile to pursue it to see whether the binary cluster approximation holds. In this connection, we comment on recent work by Sanchez.[56] He claims that A_2 for monodisperse polymers is proportional to $M^{-1/2}$ near Θ if higher cluster integrals are taken into account by the mean field theory, i.e., the smooth-density model in polymer solution terminology. However, this approach was rejected by Yamakawa[57] long ago, since he found that the smooth-density model led to an erroneous molecular weight dependence of the expansion factor and A_2 for monodisperse polymers when the ternary cluster integral was introduced. The same defect of the mean field theory was pointed out recently by de Gennes.[58]

Now we turn to the effects of heterogeneity on A_2. In Figures 5 and 6, the ratios A_2^{OS}/A_2^{LS} are plotted against M_w/M_n for polymers with Schulz-Zimm and log-normal distributions. The numbers attached to the curves indicate the values of z_w. For both cases, A_2^{OS} for a given polymer is greater than A_2^{LS} at all values of M_w/M_n, in agreement with the hard-sphere theory.[59] But for very large values of M_w/M_n, the ratio A_2^{OS}/A_2^{LS} tends to some finite value, depending on z_w, and contradicts the hard-sphere result, which gives $A_2^{OS}/A_2^{LS} \propto M_w/M_n$ in the limit for $M_w/M_n \to \infty$. One interesting feature of the log-normal distribution is that the ratio is most sensitive to z_w at low values of this parameter, say, for $z_w < 1$, while at higher values it approaches its asymptote for large z_w very rapidly. On the scale of Figure 6, there is no difference between curves for $z_w = 10$ and 50. In polymers with a Schulz-Zimm

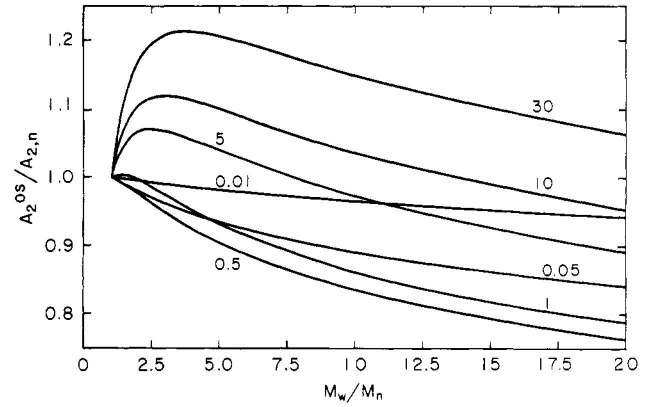

Figure 7. $A_2^{OS}/A_{2,n}$ plotted against M_w/M_n for polymers with a Schulz-Zimm distribution. The attached numbers indicate values of z_w.

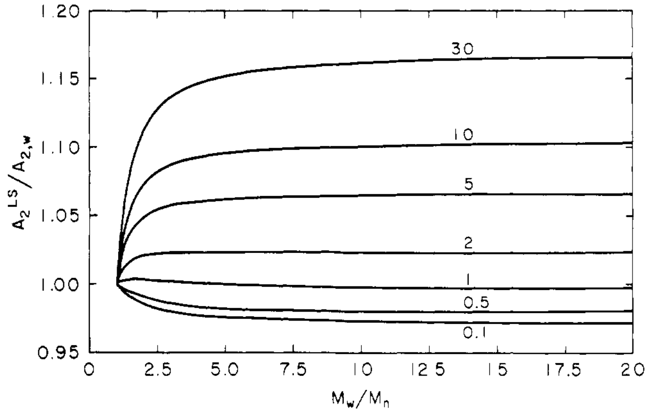

Figure 8. $A_2^{LS}/A_{2,w}$ plotted against M_w/M_n for polymers with a Schulz-Zimm distribution. The attached numbers indicate values of z_w.

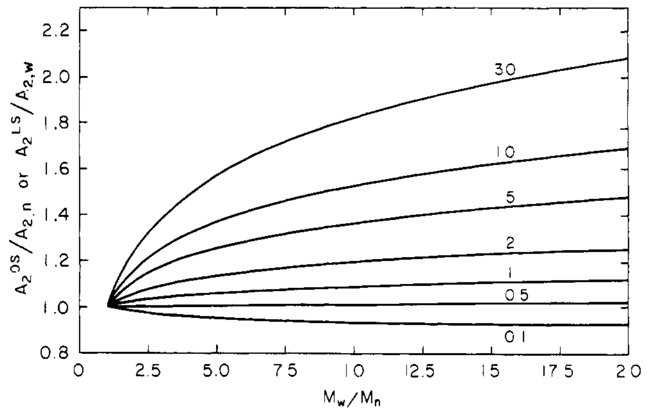

Figure 9. $A_2^{OS}/A_{2,n}$ or $A_2^{LS}/A_{2,w}$ plotted against M_w/M_n for polymers with a log-normal distribution. The attached numbers indicate values of z_w.

distribution, on the other hand, the ratio keeps growing even for very high values of z_w.

Next we compare the virial coefficients of polydisperse polymers with those for monodisperse polymers. In Figures 7–9, ratios $A_2^{OS}/A_{2,n}$ and $A_2^{LS}/A_{2,w}$ are shown for the two distributions. Here, $A_{2,n}$ and $A_{2,w}$ are the second virial coefficients for monodisperse polymers with molecular weights equal to the number-average and weight-average molecular weights of corresponding heterogeneous polymers, respectively. We note that the two ratios $A_2^{OS}/A_{2,n}$ and $A_2^{LS}/A_{2,w}$ are identical for polymers with a log-normal distribution (see Appendix D). The figures attached to the curves indicate z_w. For small values of this parameter the ratios decrease with increasing M_w/M_n for both distributions. At higher values of z_w, the ratios monotonously increase with M_w/M_n, except for $A_2^{OS}/A_{2,n}$ for a Schulz–Zimm distribution, which exhibits a maximum. The effect of solvent power on the ratios is greater for the log-normal distribution than for the Schulz–Zimm distribution. For most practical cases, however, z_w is less than 5, and the effects of heterogeneity on the ratios may well be within the limits of experimental error.

Combining several "monodisperse" polymers, Elias, Bellido, and Bareiss[60] prepared mixtures with the intention to mimic the Schulz–Zimm and log-normal distributions. However, their data are not compared with the present theory since they contain some obvious inconsistencies: (1) data for the samples with the log-normal distribution strongly deviate from the exact relation $A_2^{OS}/A_{2,n} = A_2^{LS}/A_{2,w}$ (eq D1); (2) values of the ratio $A_2^{OS}/A_{2,n}$ reach as low as 0.4 with $M_w/M_n = 2.1$, which is well below the lower bound for the Schulz–Zimm distribution given by

$$A_2^{OS}/A_{2,n} \geq h^a\Gamma(h + 1 - a)/\Gamma(h + 1) \qquad (49)$$

Here, eq 49 is derived by using the inequality $A_{ij} \geq (A_{ii} + A_{jj})/2$ that follows from the free energy discussion above, and by assuming the power law $A_{ii} = \text{const} \times M_i^{-a}$. With $1 \leq M_w/M_n \leq 3$ and $a = 0.2$ corresponding to their samples, eq 40 gives $A_2^{OS}/A_{2,n} \geq 0.88$.

Acknowledgment. This work was supported by the National Science Foundation under Grant No. DMR-7919422. We are grateful to Professors W. H. Stockmayer and H. Fujita for their helpful comments.

Added Note

We were unaware until recently of a related study by Straube and Oeltze.[61] Citing that work, one of the reviewers of this paper pointed out that experimental results in ref 12 show a tendency to a decrease in maxima of A_2^{OS} and A_2^{LS} for $\epsilon > 10$, as suggested by the Straube–Oeltze theory but contrary to our results. With regard to this we comment as follows: First, Straube and Oeltze used among others the factorization approximation to the conditional probability density for segment contacts, which yields the Casassa–Markovitz–Fixman equation[3] for A_{11}. Since the treatment contains only the effect of double contacts, the logarithmic term $\ln \epsilon$ arising from triple-contact correlations between inter- and intramolecular interactions is lost. In our opinion, it is the absence of this term in the Straube–Oeltze theory that is responsible for the difference in predicted behavior, since the logarithmic term becomes particularly important in the asymptote for $\epsilon \to \infty$. Second, the data in ref 12 clearly show the experimental difficulties encountered in obtaining accurate values for A_2. For instance, the ratios A_2^{OS}/A_2^{LS} obtained for "monodisperse" polymers ($M_w/M_n \lesssim 1.05$) are around 1.2–1.4. Large deviations from unity are inconsistent with the reported low polydispersity of samples and suggest relatively large experimental errors in determination of A_2 or M, or both. Summarizing the above, we do not believe that the decrease in maxima of A_2 for $\epsilon > 10$ indeed occurs.

As a matter of fact, it is generally recognized that it may be very difficult to accurately extract the true second virial coefficients from experimental data. The crossover from virial series to the noninteger power dependence of the osmotic pressure can be broad and start at low concentrations. Even if this is not the case, the determination of A_2 is often hampered by the effect of higher virial terms whose magnitude is not known.

Appendix A. Integral I_2

I_2 is a contribution to $C_2(\epsilon)$ of a cluster whose interaction determinant cannot be diagonalized. It may be written as

$$\begin{aligned} I_2 = 4\epsilon^2 \int_0^1 \int_0^1 \int_{u=0}^{s} \int_{v=0}^{t} & \frac{(1-s)(1-t)}{[(u+\epsilon v)(s-u+\epsilon t-\epsilon v)+\epsilon uv]^{3/2}} \, \mathrm{d}s \, \mathrm{d}t \, \mathrm{d}u \, \mathrm{d}v = \\ & 16\left[\left(1+\frac{1}{3\epsilon}\right)S_1(\epsilon) + \left(\frac{\epsilon^2}{3}+\epsilon\right)S_1(\epsilon^{-1})\right] + \\ & \frac{5\pi}{\epsilon} - 4\epsilon^{1/2}\left(\epsilon+\frac{1}{\epsilon}\right) + \\ & \frac{(1+\epsilon)^3}{3\epsilon}\left\{\frac{11}{3}\left[4 \operatorname{Arctan} \epsilon^{-1/2} - \operatorname{Arctan} \frac{2(2\epsilon-1)}{\epsilon^{1/2}(4\epsilon+7)} - \right.\right. \\ & \left.\left.\operatorname{Arctan} \frac{2(2\epsilon-1)}{\epsilon^{1/2}(\epsilon-5)}\right] - 4S_2(\epsilon)\right\} + \\ & \left(\frac{74}{9}\epsilon^2 - \frac{14}{3}\epsilon - \frac{14}{3} - \frac{16}{9\epsilon}\right) \operatorname{Arctan} \frac{1}{2\epsilon^{1/2}} + \\ & \left(\frac{16}{9}\epsilon^2 + \frac{14}{3}\epsilon + \frac{14}{3} - \frac{74}{9\epsilon}\right) \operatorname{Arctan} \frac{2}{\epsilon^{1/2}} \end{aligned} \qquad \text{(A1)}$$

where $S_1(\epsilon)$ and $S_2(\epsilon)$ are single integrals defined as

$$S_1(\epsilon) = \int_0^{\epsilon^{1/2}} x^{-1} \operatorname{Arctan} \frac{x}{1+2x^2} \, \mathrm{d}x \qquad \text{(A2)}$$

$$S_2(\epsilon) = \int_0^1 x^{-1} f(\epsilon x, 1+\epsilon) \, \mathrm{d}x \qquad \text{(A3)}$$

with

$$f(x,y) = \operatorname{Arcsin} \frac{y + x(1+y) - x^2}{[(y-x)(y+3x)]^{1/2}(1+x)} - \operatorname{Arcsin}\left(\frac{y-x}{y+3x}\right)^{1/2} \qquad \text{(A4)}$$

Appendix B. Asymptotic Form of $C_2(\epsilon)$

As apparent from the form of I_2, the complete coefficient $C_2(\epsilon)$, which is a sum of similar terms, is too complicated to be of any practical use. To approximate it by a simpler formula, we studied its asymptotic form. $C_2(\epsilon)$ is a sum of eight integrals

$$C_2(\epsilon) = \sum_{j=1}^{8} I_j \qquad \text{(B1)}$$

Explicit forms of the I_j's except I_2 are found in Tagami–Casassa's paper. Expanding all I_j's up to ϵ^{-1}, we have

$$I_1 = 4\pi - \frac{256}{15\epsilon^{1/2}} + 4\pi\epsilon^{-1} - \ldots$$

$$I_2 = 8\pi \ln 2 - \frac{128}{5\epsilon^{1/2}} + \left(5 + \frac{8}{3} \ln 2\right)\pi\epsilon^{-1} - \ldots$$

$$I_3 = 8 - 2\pi - \left(2\pi - \frac{16}{3}\right)\epsilon^{-1} - \ldots$$

$$I_4 = 4 \ln \epsilon - 2\pi - 6 + 8 \ln 2 + \frac{128}{15\epsilon^{1/2}} - \left(2\pi - \frac{1}{3} - 4 \ln 2\epsilon^{1/2}\right)\epsilon^{-1} + \ldots$$

$$I_5 = \pi - \frac{8}{3} - \frac{8}{5\epsilon^{1/2}} + \left(\frac{\pi}{12} - \frac{16}{45}\right)\epsilon^{-1} + \ldots \qquad \text{(B2)}$$

$$I_6 = 4 \ln \epsilon - 4\pi - 6 + 8 \ln 2 + \frac{128}{5\epsilon^{1/2}} - \left(\frac{16}{3}\pi - \frac{17}{9} + \frac{4}{3} \ln 2\epsilon^{1/2}\right)\epsilon^{-1} + \ldots$$

$$I_7 = 16 - 8\pi\left(1 - \ln \frac{3}{2}\right) - \left(\frac{7\pi}{3} - \frac{32}{9} - \frac{8\pi}{3} \ln \frac{3}{2}\right)\epsilon^{-1} + \ldots$$

$$I_8 = (4\pi - 8) \ln \epsilon + 10\pi - 4 - 16 \ln 2 - 8\pi \ln 3 + \frac{256}{15\epsilon^{1/2}} - \left(\frac{2\pi}{9} + \frac{10}{9} + \frac{8\pi}{3} \ln 3 + \frac{8}{3} \ln 2\epsilon^{1/2} - \frac{4\pi}{3} \ln \epsilon\right)\epsilon^{-1} + \ldots$$

The leading terms of all I_j's except for I_2 agree with those given by Tagami and Casassa.[21] Substituting eq B2 into eq B1, we obtain

$$C_2(\epsilon) = \pi(4 \ln \epsilon - 1) + \frac{16}{3} + \frac{104}{15}\epsilon^{-1/2} + \left(\frac{4\pi}{3} \ln \epsilon - \frac{101\pi}{36} + \frac{437}{45}\right)\epsilon^{-1} + \mathcal{O}(\epsilon^{-3/2}) \qquad \text{(B3)}$$

The leading term stays the same, but the constant and higher order terms in $\epsilon^{-n/2}$ differ from the previously reported values.[21]

For intermolecular interactions only, we have from I_1 and I_2

$$C_2{}^0(\epsilon) = 4\pi(1 + 2 \ln 2) - \frac{128}{3\epsilon^{1/2}} + \pi\left(9 + \frac{8}{3} \ln 2\right)\epsilon^{-1} + \mathcal{O}(\epsilon^{-3/2}) \qquad \text{(B4)}$$

Appendix C. Numerical Integration

All numerical work has been done with a Hewlett-Packard 2117-F computer. The single integrals appearing in I_2, I_7, and I_8 were evaluated by Gaussian quadrature.

Since Tagami and Casassa[21] have pointed out that computed values of these integrals grow as the number of interval subdivisions increases, we investigated this point carefully. For the integrals in I_7 and I_8, their original variable, y, is replaced by $x = y^{1/2}$. Then the integrand stays finite even at the integration limits, and the integrals are evaluated accurately with a lesser number of subdivisions. We also transformed Arcsin into Arctan to save computer time. Values calculated this way are almost constant for 16–64-point Gaussian quadrature. In the worst case we observed, they changed by 0.001% at ϵ = 100 and 0.006% at ϵ = 1000. However, this range of very high ϵ is very well described by the asymptotic formula, and the integrals are no longer needed. Similar considerations apply to S_1 and S_2 evaluation for the I_2 integral. Values of I_2 obtained from eq A1 were compared with those evaluated by a two-dimensional quadrature

$$I_2 = 16\epsilon \int_0^1 \int_0^1 f(x,\epsilon^{1/2}y) \frac{(1 - x^2)(1 - y^2)xy}{x^2 + \epsilon y^2} \, \mathrm{d}x \, \mathrm{d}y \qquad \text{(C1)}$$

where

$$f(x,y) = 2\left(\text{Arctan } \frac{xy}{x^2 + 2y^2} + \text{Arctan } \frac{2x}{y}\right) - \left(\text{Arctan } \frac{x(4x^2 + 7y^2)}{2y(2x^2 - y^2)} + \text{Arctan } \frac{x(x^2 - 5y^2)}{2y(2x^2 - y^2)}\right) \qquad \text{(C2)}$$

Here $(2N,2N)$-point Gaussian quadratures were used with N = 64. The two results differ by 0.0002% at ϵ = 10, 0.004% at ϵ = 50, and 0.01% at ϵ = 100.

Appendix D. Second Virial Coefficients for Polymers with Log-Normal Distribution

The purpose of this appendix is to show that

$$A_2{}^{\mathrm{OS}}/A_{2,\mathrm{n}} = A_2{}^{\mathrm{LS}}/A_{2,\mathrm{w}} \qquad \text{(D1)}$$

if the polymer has a log-normal type of molecular weight distribution.

Substituting eq 40 with eq 41 and 42 into eq 5 and replacing the sums by integration followed by a change of variable, we have

$$A_2{}^{\mathrm{OS}} = \pi^{-1} \int_{-\infty}^{\infty} \int_{-\infty}^{\infty} A(M_\mathrm{n} e^{\sigma^2/2 + 2^{1/2}\sigma X}, M_\mathrm{n} e^{\sigma^2/2 + 2^{1/2}\sigma Y}) e^{-X^2 - Y^2} \, \mathrm{d}X \, \mathrm{d}Y \qquad \text{(D2)}$$

where we use notation $A_{ij} \equiv A(M_i,M_j)$. $A_{2,\mathrm{n}}$ is obtained in the limit of $\sigma \rightarrow 0$ with M_n fixed:

$$A_{2,\mathrm{n}} = \lim_{\substack{\sigma \to 0 \\ M_\mathrm{n} \text{ fixed}}} A_2{}^{\mathrm{OS}} = A(M_\mathrm{n},M_\mathrm{n}) \qquad \text{(D3)}$$

Thus, the ratio $A_2{}^{\mathrm{OS}}/A_{2,\mathrm{n}}$ is written as

$$A_2{}^{\mathrm{OS}}/A_{2,\mathrm{n}} = [\pi A(M,M)]^{-1} \int_{-\infty}^{\infty} \int_{-\infty}^{\infty} A(M e^{\sigma^2/2 + 2^{1/2}\sigma X}, M e^{\sigma^2/2 + 2^{1/2}\sigma Y}) e^{-X^2 - Y^2} \, \mathrm{d}X \, \mathrm{d}Y \qquad \text{(D4)}$$

Similarly, eq 6 and 40 with eq 41 and 42 yield the right-hand side of eq D2 for $A_2{}^{\mathrm{LS}}$, with M_n replaced with M_w. This establishes the equality D1.

References and Notes

(1) McMillan, W. G.; Mayer, J. E. *J. Chem. Phys.* **1945**, *13*, 276.
(2) Zimm, B. H. *J. Chem. Phys.* **1946**, *14*, 164.
(3) Yamakawa, H. "Modern Theory of Polymer Solutions"; Harper and Row: New York, 1971.
(4) Krigbaum, W. R.; Flory, P. J. *J. Am. Chem. Soc.* **1953**, *75*, 1775.
(5) Chien, J.-Y.; Shih, L.-H.; Yu, S.-C. *J. Polym. Sci.* **1958**, *29*, 117.
(6) Varadaiah, V. V.; Rao, V. S. *J. Polym. Sci.* **1961**, *50*, 31.
(7) Casassa, E. F.; Stockmayer, W. H. *Polymer* **1962**, *3*, 53.
(8) Kato, T.; Miyaso, K.; Nagasawa, M. *J. Phys. Chem.* **1968**, *72*, 2161.
(9) Utiyama, H.; Tagata, N.; Kurata, M. *J. Phys. Chem.* **1969**, *73*, 1448.
(10) Wallace, T. P.; Casassa, E. F. *Polym. Prepr., Am. Chem. Soc., Div. Polym. Chem.* **1970**, *11*, 136.
(11) Suzuki, H. *Br. Polym. J.* **1977**, *9*, 222.
(12) Noda, I.; Kitano, T.; Nagasawa, M. *J. Polym. Sci., Polym. Phys. Ed.* **1977**, *15*, 1129.
(13) Flory, P. J.; Krigbaum, W. R. *J. Chem. Phys.* **1950**, *18*, 1086.
(14) Casassa, E. F. *Polymer* **1960**, *1*, 169.
(15) Orofino, T. A.; Flory, P. J. *J. Chem. Phys.* **1957**, *26*, 1067.
(16) Stockmayer, W. H. *Makromol. Chem.* **1960**, *35*, 54.
(17) Stockmayer, W. H. *Br. Polym. J.* **1977**, *9*, 89.

(18) Tanaka, G. *J. Polym. Sci., Polym. Phys. Ed.* **1979**, *17*, 305.
(19) Tanaka, G. *Macromolecules* **1980**, *13*, 1513.
(20) Yamakawa, H.; Kurata, M. *J. Chem. Phys.* **1960**, *32*, 1852.
(21) Tagami, Y.; Casassa, E. F. *J. Chem. Phys.* **1969**, *50*, 2206.
(22) Kirkwood, J. G.; Goldberg, R. J. *J. Chem. Phys.* **1950**, *18*, 54.
(23) Stockmayer, W. H. *J. Chem. Phys.* **1950**, *18*, 58.
(24) Koningsveld, R.; Stockmayer, W. H.; Kennedy, J. W.; Kleintjens, L. A. *Macromolecules* **1974**, *7*, 73.
(25) Kleintjens, L. A.; Koningsveld, R.; Stockmayer, W. H. *Br. Polym. J.* **1976**, *8*, 144.
(26) Kurata, M. "Thermodynamics of Polymer Solutions"; MMI Press: Midland, MI, 1982.
(27) Flory, P. J. "Principles of Polymer Chemistry"; Cornell University Press: Ithaca, NY, 1953.
(28) Huggins, M. L. "Physical Chemistry of High Polymers"; Wiley: New York, 1958.
(29) Tompa, H. *C. R. Reun. Chim. Phys.*, Paris, 1952.
(30) Fujita, H.; Teramoto, A. In "Polymer Compatibility and Incompatibility"; Šolc, K., Ed.; MMI Press: Midland, MI, 1982; p 125.
(31) Albrecht, A. C. *J. Chem. Phys.* **1957**, *27*, 1002.
(32) Yamakawa, H. *J. Phys. Soc. Jpn.* **1958**, *13*, 87.
(33) Kurata, M.; Yamakawa, H. *J. Chem. Phys.* **1958**, *29*, 311.
(34) Kurata, M.; Fukatsu, M.; Sotobayashi, H.; Yamakawa, H. *J. Chem. Phys.* **1964**, *41*, 139.
(35) Schulz, G. V. *Z. Phys. Chem., Abt. B* **1939**, *43*, 25.
(36) Zimm, B. H. *J. Chem. Phys.* **1948**, *16*, 1093, 1099.
(37) Wesslau, H. *Makromol. Chem.* **1956**, *20*, 111.
(38) Stroud, A. H.; Secrest, D. "Gaussian Quadrature Formulas"; Prentice-Hall: Englewood Cliffs, NJ, 1966.
(39) Yamakawa, H. *J. Chem. Phys.* **1968**, *48*, 2103.
(40) Stockmayer, W. H.; Fixman, M. *J. Polym. Sci., Part C* **1963**, *1*, 137.
(41) Tanaka, G.; Imai, S.; Yamakawa, H. *J. Chem. Phys.* **1970**, *52*, 2639.
(42) Yamakawa, H. *Pure Appl. Chem.* **1972**, *31*, 179.
(43) Berry, G. C. *J. Chem. Phys.* **1966**, *44*, 4550.
(44) Berry, G. C. *J. Chem. Phys.* **1967**, *46*, 1338.
(45) Yamamoto, A.; Fujii, M.; Tanaka, G.; Yamakawa, H. *Polym. J.* **1971**, *2*, 799.
(46) Fukuda, M.; Fukutomi, M.; Kato, Y.; Hashimoto, T. *J. Polym. Sci., Polym. Phys. Ed.* **1974**, *12*, 871.
(47) Miyaki, Y.; Einaga, Y.; Fujita, H. *Macromolecules* **1978**, *11*, 1180.
(48) Outer, P.; Carr, C. I.; Zimm, B. H. *J. Chem. Phys.* **1954**, *18*, 830.
(49) Kato, T.; Miyaso, K.; Noda, I.; Fujimoto, T.; Nagasawa, M. *Macromolecules* **1970**, *3*, 777.
(50) Matsumoto, T.; Nishioka, N.; Fujita, H. *J. Polym. Sci., Part A2* **1972**, *10*, 23.
(51) Chinai, S. N.; Matlack, J. D.; Resnick, A. L.; Samuels, R. J. *J. Polym. Sci.* **1955**, *17*, 391.
(52) Schulz, G. V.; Cantow, H.-J.; Meyerhoff, G. *J. Polym. Sci.* **1953**, *10*, 79.
(53) Cohen-Ginsberg, E.; Fox, T. G; Mason, H. F. *Polymer* **1962**, *3*, 97.
(54) Koningsveld, R. Thesis, Leiden University, 1967.
(55) Tompa, H. *Trans. Faraday Soc.* **1949**, *45*, 1142.
(56) Sanchez, I. C. *Ferroelectrics* **1980**, *30*, 7.
(57) Yamakawa, H. *J. Chem. Phys.* **1966**, *45*, 2606.
(58) de Gennes, P.-G. "Scaling Concepts in Polymer Physics"; Cornell University Press: Ithaca, NY, 1979.
(59) Casassa, E. F. *Polymer* **1962**, *3*, 625.
(60) Elias, H.-G.; Bellido, J.; Bareiss, R. E. *Makromol. Chem.* **1975**, *176*, 439.
(61) Straube, E.; Oeltze, K. *Acta Polym.* **1979**, *30*, 623.

Theory of Elasticity of Polymer Networks. 3

Paul J. Flory* and Burak Erman†

IBM Research Laboratory, San Jose, California 95193, and Department of Chemistry, Stanford University, Stanford, California 94305.

Received November 17, 1981

ABSTRACT: The theory of elasticity of polymer networks is reformulated with greater generality and improved concision. In particular, the domains of constraint that, due to entanglements and steric requirements of real polymer chains, impede fluctuations of the junctions are introduced in a way that admits of a more rapid attenuation of these constraints than affine transformation of them with strain would allow. Illustrative calculations are presented on the contribution of the constraints to the stress in uniaxial deformation as a function of the extension ratio and the degree of dilation. The calculated reduced force is decidedly nonlinear with the reciprocal of the extension ratio.

Introduction

The elastic free energy of a polymer network that exhibits high elasticity can be expressed as the sum of two terms.[1–3] One represents the elastic free energy ΔA_{ph} of the hypothetical phantom network that is topologically identical with the real one. The other, ΔA_c, is due to the constraints arising from the material properties of real chains densely interspersed in the random network. Thus,

$$\Delta A_{\mathrm{el}} = \Delta A_{\mathrm{ph}} + \Delta A_c \qquad (1)$$

A phantom network is, by definition,[4] one in which the physical effects of the chains between junctions are confined exclusively to the forces they exert on the pairs of junctions to which each is attached. Neither the space-filling characteristics of real chains nor the structural integrity that precludes transection of one chain by another is considered to be operative in the phantom network. The forces delivered to the junctions by the chains originate in the configurational-statistical characteristics of the chains as expressed, for example, in the distribution $W(\mathbf{r})$ of end-to-end vectors $\mathbf{r}$ for chains free of constraints. For chains of the lengths that are usual in representative elastomeric networks, $W(\mathbf{r})$ is Gaussian in good approximation.[5–7] The elastic free energy of a phantom network of Gaussian chains is given rigorously by[4,8]

$$\Delta A_{\mathrm{ph}} = (1/2)\xi kT(\lambda_1^2 + \lambda_2^2 + \lambda_3^2 - 3) \qquad (2)$$

where λ_1, λ_2, and λ_3 are principal extension ratios relative to the isotropic state of reference in which the chains assume random configurations corresponding to those of unperturbed, free chains, k is the Boltzmann constant, and ξ is the cycle rank of the network, or the number of independent circuits it contains.[4] With ξ thus defined, eq 2 holds for phantom networks of any functionality and irrespective of their structural imperfections.

In typical polymer networks that exhibit high elasticity the space pervaded by one chain is shared with many others and their associated junctions.[1,4] The degree of interpenetration is high. For illustration, consider the

---

[†] Permanent address: School of Engineering, Bogazici University, Bebek, Istanbul, Turkey.

0024-9297/82/2215-0800$01.25/0